crystals

MDPI

*Article*

# Wear Characterization of Laser Cladded Ti-Nb-Ta Alloy for Biomedical Applications

**Raj Soni [1], Sarang Pande [1,*], Santosh Kumar [2], Sachin Salunkhe [3], Harshad Natu [4] and Hussein Mohammed Abdel Moneam Hussein [5,6]**

1 Department of Mechanical Engineering, Marwadi University, Rajkot 360003, India
2 Department of Mechanical Engineering, Indian Institute of Technology, Varanasi 221005, India
3 Department of Mechanical Engineering, Vel Tech Rangarajan Dr. Sagunthala R & D Institute of Science and Technology, Chennai 600062, India
4 Magod Fusion Technologies Pvt. Ltd., Pune 411026, India
5 Mechanical Engineering Department, Faculty of Engineering and Technology, Future University in Egypt, New Cairo 11835, Egypt
6 Mechanical Engineering Department, Faculty of Engineering, Helwan University, Cairo 11732, Egypt
* Correspondence: sarang.pande@marwadieducation.edu.in

**Abstract:** Additive manufacturing (AM) has started to unfold diverse fields of applications by providing unique solutions to manufacturing. Laser cladding is one of the prominent AM technologies that can be used to fulfill the needs of custom implants. In this study, the wear resistance of the laser cladded titanium alloy, Ti-17Nb-6Ta, has been evaluated under varied loads in Ringer's solution. Microstructural evaluation of the alloy was performed by SEM and EDX, followed by phase analysis through XRD. The wear testing and analysis have been carried out with a tribometer under varied loads of 10, 15, and 20 N while keeping other parameters constant. Abrasion was observed to be the predominant mechanism majorly responsible for the wearing of the alloy at the interface. The average wear rate and coefficient of friction values were 0.016 $mm^3$/Nm and 0.22, respectively. The observed values indicated that the developed alloy exhibited excellent wear resistance, which is deemed an essential property for developing biomedical materials for human body implants such as artificial hip and knee joints.

**Keywords:** Ti alloys; β-phase; laser cladding; wear characterization; biomedical applications



**Citation:** Soni, R.; Pande, S.; Kumar, S.; Salunkhe, S.; Natu, H.; Hussein, H.M.A.M. Wear Characterization of Laser Cladded Ti-Nb-Ta Alloy for Biomedical Applications. *Crystals* **2022**, *12*, 1716. https://doi.org/10.3390/cryst12121716

Academic Editors: Yang Zhang and Yuqiang Chen

Received: 20 September 2022
Accepted: 16 October 2022
Published: 25 November 2022



## 1. Introduction

Over the years, there has been a growing need for hard-tissue replacements in the human body like hip/knee joints, teeth, etc., [1]. Some of the key reasons are attributable to the increasing age of the population and increased life expectancy due to better health care in the past decades [2]. A high number of accidents also increases the demand [3]. Due to this, interest has surged in exploring the possibilities for the materials that fulfil the replacement needs. Metallic materials are outstanding hard-tissue replacement materials because of their versatile properties like high mechanical strength, toughness, and promising biocompatibility [4]. Titanium (Ti) alloys possess the required properties like high strength, outstanding biocompatibility, low density, enhanced resistance to corrosion, etc., making them a perfect candidate for use in the human body [5,6]. One of the critical reasons for Ti and its alloys' outstanding biological and physical properties is the presence of an oxide film ($TiO_2$), which is generated naturally on their surface [7]. However, the low hardness and wear resistance affect their full flange use [8]. The ASTM standardized Ti alloy Ti-6Al-4V has high resistance to corrosion, excellent machinability, and tensile strength [9,10]. However, due to a mismatch in Young's modulus (~110 GPa) compared to the human bone (~30 GPa) and reported claims of creating severe health problems such as

adverse tissue reactions and neurological disorders [11,12], there has been renewed interest in the search for its alternatives for use in biomedical applications.

Titanium is an allotropic element present in various phases like α, α + β, and β. α-stabilizers and β-stabilizers are added to enhance the α- and β-phases, respectively [13]. Over the past years, numerous studies have been conducted in search of β-Ti alloys, which potentially possess desired mechanical properties and resistance to corrosion. Due to the drawback of Al- and V- ions in Ti-6Al-4V, past studies have tried replacing those elements with other β-stabilizers such as Ta, Sn, Mo, Nb, and Zr to make β-Ti alloys [14,15]. Wei et al. [16] examined Ti-Ta-Nb alloys with 15, 23, and 30 Ta mass% for evaluating the microstructural, biocompatibility, and mechanical properties. Ti-30Ta-10Nb was the optimum alloy, with a Young's modulus of around 60 GPa, a strength of around 1250 MPa, and a hardness of around 3.1 GPa. A Ti-23Ta-10Nb alloy, was also suitable with a Young's modulus of around 75 GPa, hardness of around 3.0 GPa, overall strength of around 1300 MPa, and favorable biocompatibility. The porous foams of this alloy exhibited strength and Young's modulus values of around 180 MPa and 10 GPa, respectively, which were observed to be close to human bone properties.

## 2. Wear in Ti Alloys

Ti alloys possess low thermal conductivity and low resistance to plastic shearing. Hence, the frictional heat keeps the mating materials attached [17]. Wear resistance is an essential property for implants, and Ti alloys are often used in mechanical joints. When these alloys are used for implant applications such as hip or knee joint replacements, their efficiency may be lower because of the sliding or slight amplitude movement generated from frictional wear [18]. This can create wear debris that is abrasive and is responsible for producing metallosis and metallic allergies [18]. Past studies have tried to upgrade the wear characteristics of Ti alloys by using surface improvement techniques such as PVD, CVD, ion implantation, thermal spraying, etc., [19–22]. However, it was observed that most processes were not suitable due to insufficient adhesion and layer thickness requirements, though some experimentation was done to generate an irregular surface. Irregular surfaces generate oxide layers, which increase the surface area by about 25–35%, due to which there is a noticeable improvement in osseointegration and bonding between the implant and the bone [23]. Barfeie et al. [24] reported that rough surfaces are supposed to give better osseointegration. However, the amount of roughness required for better results is still unknown.

In their study, Khan and Nisar [25] discussed the abrasive wear of a zinc-aluminum alloy. They used pin-on-disc equipment with a 1 m/s sliding speed to obtain the necessary wear characteristics. Loads of 5, 10, 15, and 20 N and 125, 250, 375, and 500 m sliding distances were chosen for the tests. Each sample was finished with up to #1200 grade SiC paper and cleaned with acetone. Increased wear with deeper grooves was noted when the applied loads were increased from 5 to 20 N.

Another study by Jing et al. [26] prepared a bio-functional gradient coating (BFGC) of hydroxyapatite (HA) on Ti6Al4V alloy samples using laser cladding. The four samples in the study were subjected to SEM, EDX, and XRD analyses, and the wear properties were evaluated in simulated body fluid (SBF). It was observed that the wear scars on the BFGC surface were very light because of the specimens' high hardness and wear resistance. The rate of wear of the grinding ball against the four specimens indirectly indicated the wear resistance of the four specimens. Overall, the abrasive wear mechanism was predominant in all four specimens.

Lee et al. [17] evaluated the wear mechanisms of untreated alloy Ti-Nb-Ta-Zr (TNTZ) and Ti-6Al-4V using a ball-on-disc type configuration in Ringer's solution and compared the results with those gained from air exposure. It was found that the volume losses ($V_{loss}$) of the TNTZ discs and balls were higher in the Ringer's solution than that of air exposure alone. Due to lower resistance to plastic shearing in the TNTZ combination, delamination wear was predominant, resulting in an excessive wear rate. On the other hand, the $V_{loss}$ of

the Ti-6Al-4V disc and ball combination decreased in Ringer's solution more than in air exposure. It may be due to the abrasive wear generated in the Ti-6Al-4V combination being effectively suppressed by Ringer's solution.

Dittrick et al. [27] evaluated the tribological behavior of laser processed Ta coatings on pure Ti and found the wear to be one order of magnitude less than pure Ti. The wear rates of pure Ti and Ta coating on Ti under 5 N load against hardened chrome steel balls were $1.39 \times 10^{-3}$ $mm^3$/Nm and $1.89 \times 10^{-4}$ $mm^3$/Nm, respectively. The authors claimed that the Ta coatings on Ti could be used in place of HA coatings for excellent wear resistance and bioactivity of human body implants.

Additive manufacturing (AM) helps in boosting the research towards making successful implants. At the same time, it fulfils the need for customization. This study tries to explore the possibilities beyond the currently used metallic biomaterials, which in turn leads to an increase in the durability of the implant and human comfort. The present study reports on the manufacturing of the Ti alloy Ti-17Nb-6Ta by laser cladding, which to the best of authors' knowledge is the first of its kind. Like titanium, metals like tantalum (Ta) and niobium (Nb) are also highly corrosion-resistant and inert in body fluids, which are responsible for enhancing the β phase as discussed earlier. XRD analysis was done to analyze the phase of the developed alloy, and microstructures were evaluated using SEM and EDX techniques. Wear characterization was carried out in Ringer's solution by varying the loads, and the friction coefficient was also obtained for the test samples. Detailed descriptions have been given in the upcoming sections.

## 3. Materials and Methods

### *3.1. Laser Cladding*

AM refers to an integral part of the industrial revolution 4.0. It is a new-age manufacturing technology that boosts research in healthcare industries in a revolutionary way. It is a digital manufacturing process that uses a computer model to fabricate the final product. Laser cladding, a leading AM process, produces net-shaped parts in a layer-by-layer pattern by using laser radiation. The three significant benefits of using laser cladding over other AM techniques are:

(1) It uses significantly less material to fabricate a product;
(2) There is no requirement to use only spherical metallic powder for manufacturing, which leads to lower final product costs [28];
(3) Gradient fabrication is possible only with this technology [29].

For large-scale acceptability of any technology, it is required that it doesn't come with any limitations. Laser cladding can be used to deposit the material on the large parts no matter what the size is, which is not seen in other AM techniques.

The setup of the laser cladding unit used in the study is illustrated in Figure 1.

For proper melting of the alloy, the minimum energy supply needed is designated as the laser energy density ($E_d$). This energy is calculated from the laser power (P), scan speed (V), and laser spot diameter (d) [30]. The relationship between the variables is represented below in Equation 1:

$$E_d = \frac{P}{Vd} \quad (1)$$

For this study, titanium powder was procured from M/s. Parshvamani Metals Pvt. Ltd., Mumbai, India. Tantalum and niobium powder were procured from M/s. Aritech Chemazone Pvt. Ltd., Kurukshetra, India. The average particle size of all the metal powders was 30–70 μm. The laser cladding for this research was performed at M/s. Magod Fusion Technologies Pvt. Ltd., Pune, India, with a 4 KW diode laser. The metal powders were mixed in a mini vertical blender in pre-set proportions (77, 17, and 6% of Ti, Nb, and Ta, respectively), followed by sieving, and then poured into a laser cladding unit. Laser cladding was performed using a 1200 W laser with a scan speed of 30 mm/s, a laser spot size of 3 mm, a powder flow rate of 12 g/min, a carrier and shielding gas velocity of 15 L/min, and a pass layer distance of 1.5 mm. Argon gas was used to maintain the

oxygen level at a low ppm to avoid contamination of the fabricated product. A pure Ti plate preheated to 200 °C was used as the substrate to ensure homogeneous cladding. The cladding was performed in a closed chamber with an inert argon atmosphere to eliminate oxidation. Post manufacturing, the samples were wire-cut into 20 mm × 20 mm × 5 mm dimensions for further characterization.

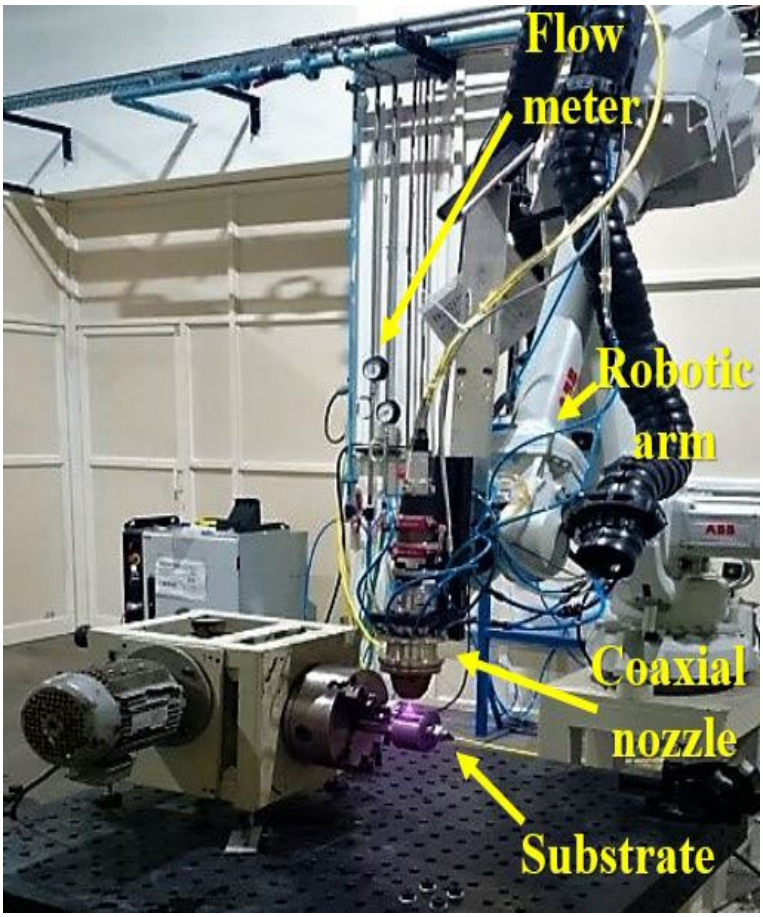


**Figure 1.** Setup of the laser cladding unit.

### *3.2. SEM, EDX, XRD, and Micro-Hardness Analyses*

SEM and EDX analyses were performed to analyze the microstructure and alloy constituents of the manufactured alloy. SEM and EDX were performed on the EVO-MA15/18SEM and 51N1000-EDS System. Following SEM and EDX, XRD analysis was conducted to analyze the phase of the manufactured alloy. The XRD analysis was done using the Rigaku Miniflex 600 Desktop XRD. For metallographic analysis, the samples were wet and finished with up to #2000 grade SiC paper. Vickers micro-hardness testing was performed on the Micro-Mach micro-hardness tester MMV-M machine.

### *3.3. Wear Testing*

A sliding wear test on the fabricated alloy was conducted using a reciprocating ball-on-disk tribometer (BioTribometer, DUCOM, Bengaluru, India) as illustrated in Figure 2. A zirconia ball of 10 mm in diameter was used. Zirconia has been used in the past in metallic parts for implant surgeries. Hence, it was chosen as a counter material for wear testing [31]. Before the testing procedure, the zirconia ball and specimens were subjected to ultrasonication for 20 min to remove any surface impurities. All the wear tests were done in a temperature-controlled environment (37 °C) using Ringer's solution as a medium. Ringer's solution was made by adding 9 g NaCl, 0.43 g KCl, 0.2 g $NaHCO_3$, and 0.24 g $CaCl_2$ to 1 L of distilled water followed by autoclaving at 121 °C for 15 min. The applied

loads were set at 10, 15, and 20 N, respectively, based on past studies [18,26,32]. The maximum Hertzian contact pressures corresponding to applied loads were 682.9, 781.7, and 860.4 MPa, respectively. The track length was 10 mm, and the frequency was 2 Hz. Each run was limited to the 1800 s. The specimens were weighed pre- and post-testing in a microelectronic balance having $10^{-3}$ g accuracy [33]. The density was calculated with the help of Archimedes' principle.

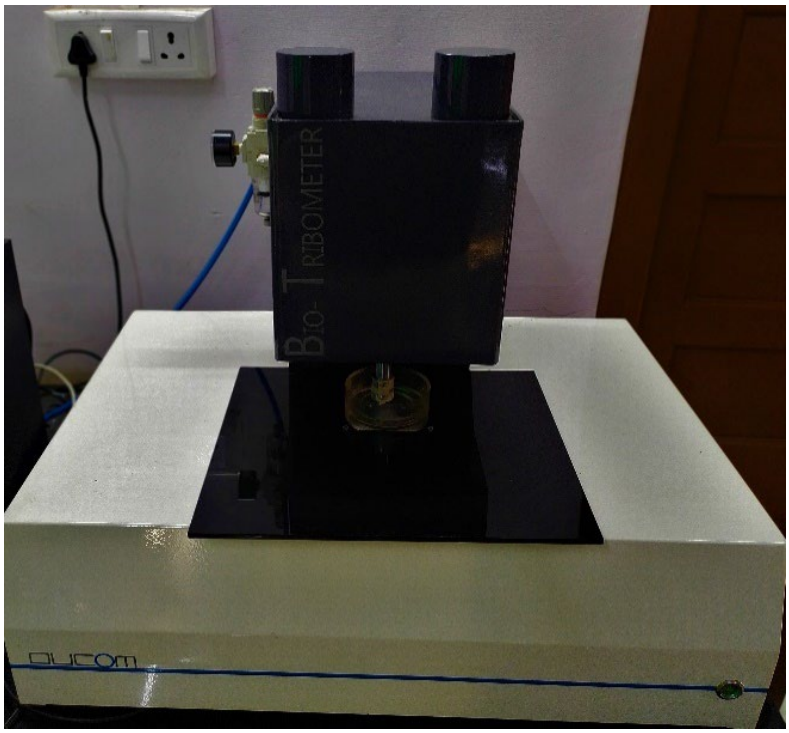


**Figure 2.** The setup of the Tribometer system.

## 4. Results and Discussion

### *4.1. SEM and EDX Analyses*

Ti, Nb, and Ta metal powders having irregular shapes are illustrated in Figure 3. SEM images delineate the pores in the fabricated alloy, which may either be due to the release of entrapped residual gases during manufacturing or to the partial evaporation of Ti from the alloy. Unmelted Ta can also be seen in the SEM images.

The EDX spectrum of the alloy in Figure 4 shows the peaks of Ti, Nb, and Ta in the manufactured alloy along with some Fe and Cu peaks in trace amounts. Fe and Cu do not affect the biomedical properties of the alloy. As a result, they can be ignored.

From EDX analysis, the proportion of each element obtained in the cladded layer is shown in Table 1.

**Table 1.** Proportion of each element in the laser cladded sample.

| | **Proportion (%)** |
|---|---|
| Ti | 75.58 |
| Nb | 15.97 |
| Ta | 5.25 |
| Fe | 2.68 |
| Cu | 0.53 |

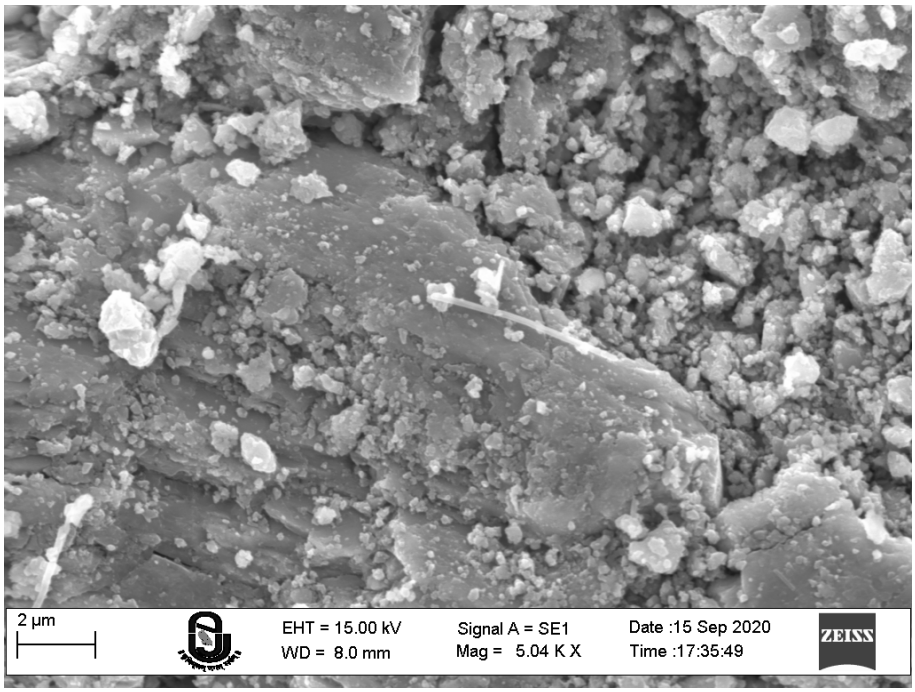


(**a**)

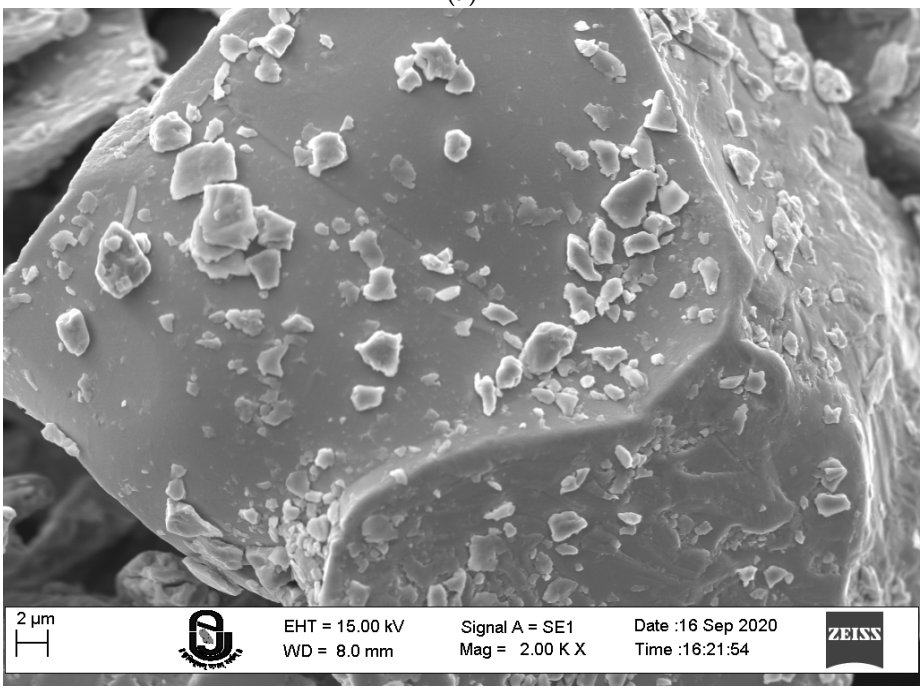


(**b**)

**Figure 3.** *Cont*.

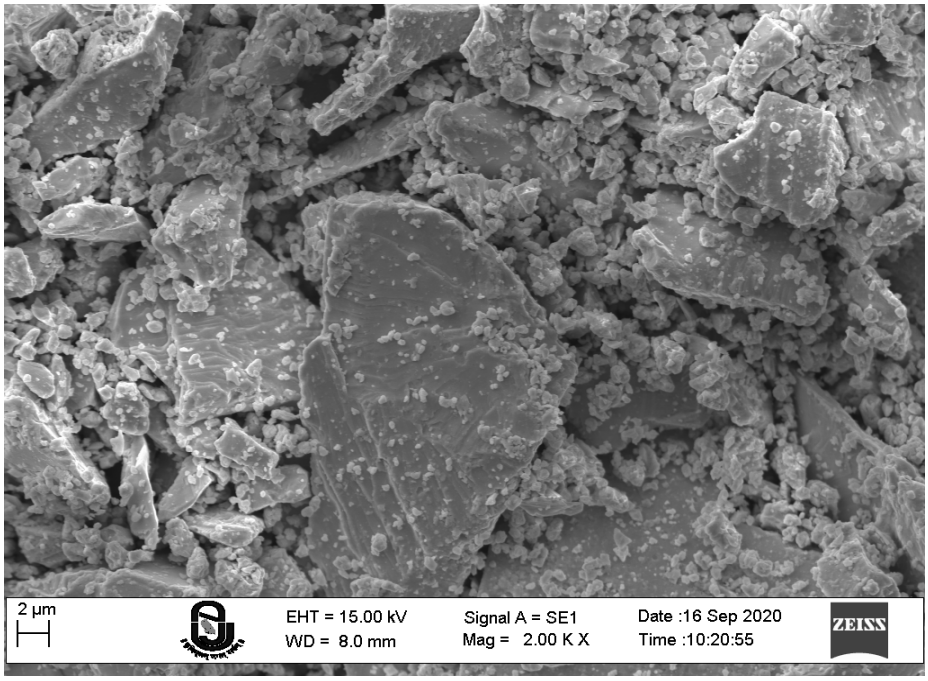


(**c**)

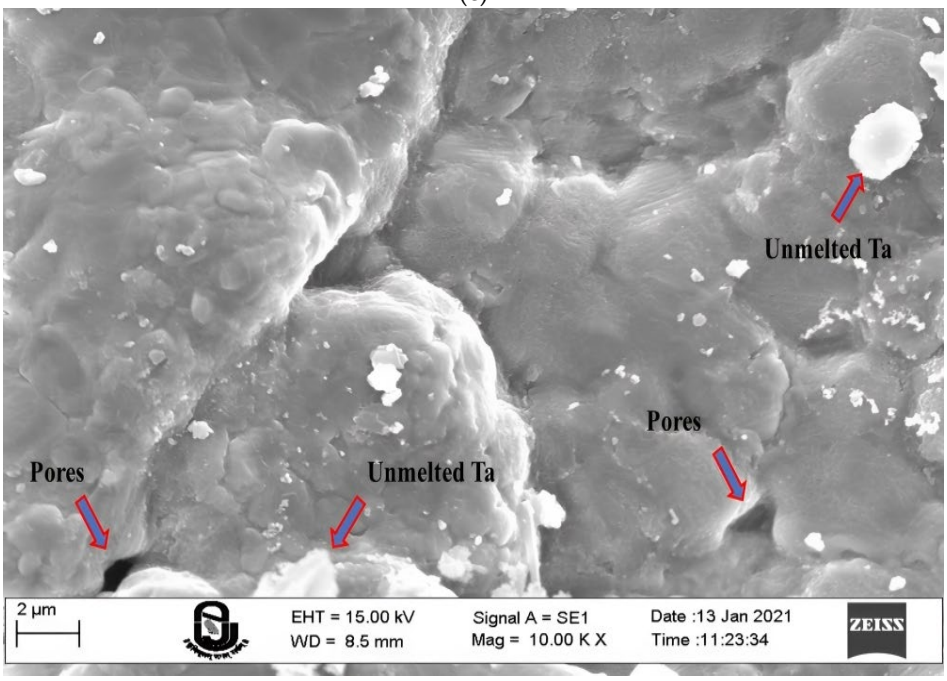


(**d**)

**Figure 3.** SEM images of (**a**) Ti, (**b**) Nb, (**c**) Ta, and (**d**) laser cladded alloy Ti-17Nb-6Ta.

The XRD spectrum of Ti-17Nb-6Ta is shown in Figure 5. The analysis was done using the X'pert Highscore and Origin Pro software. The majority of peaks belong to the BCC structure, which means that the manufactured alloy has a pure β-phase except for some small peaks which could be unrecognized due to contained impurities. The β-phase alloy possesses good wear characteristics in comparison to α or α + β alloys.

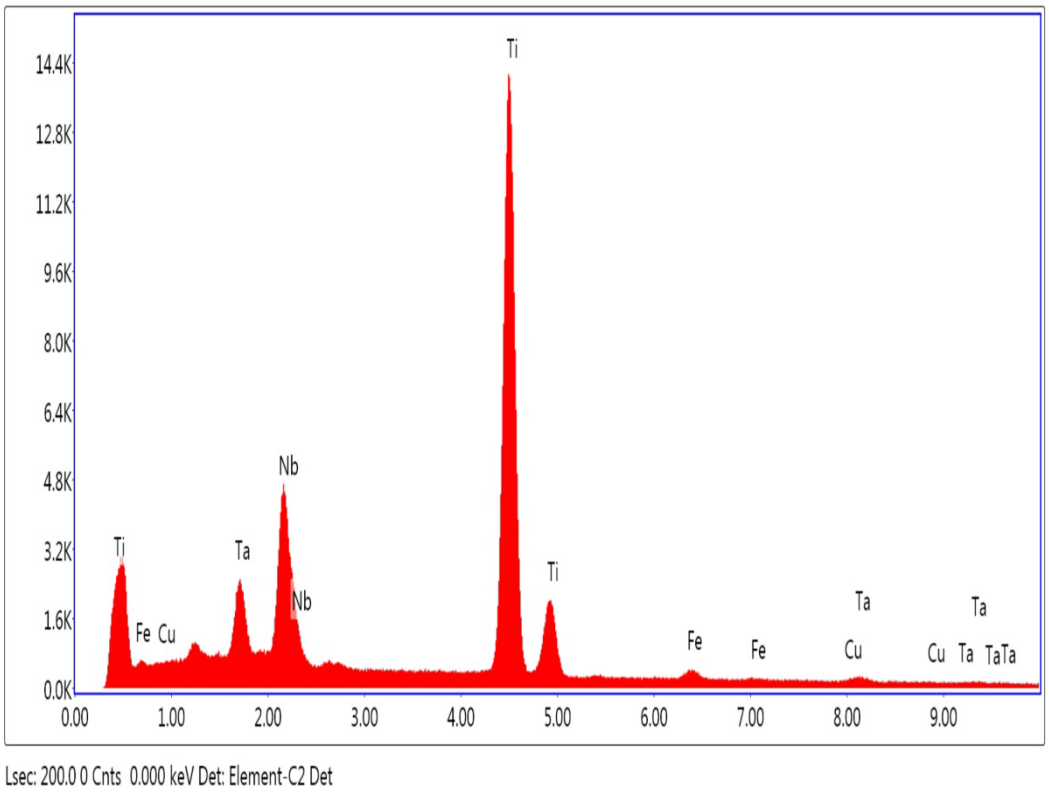


**Figure 4.** EDX spectrum of the alloy Ti-17Nb-6Ta.

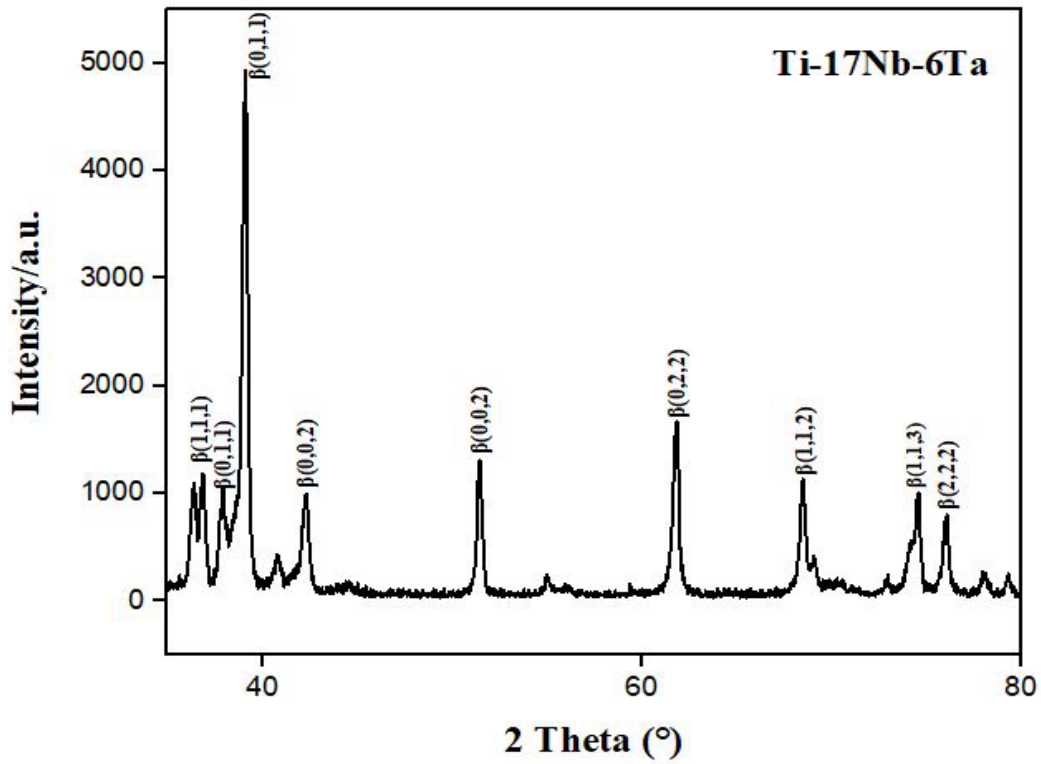


**Figure 5.** XRD spectrum of the alloy Ti-17Nb-6Ta.

### *4.2. Hardness Testing*

The laser cladded Ti-17Nb-6Ta alloy showed a micro-hardness of 176 HV, which was higher than the pure Ti substrate, which showed a hardness of 165 HV.

### *4.3. Wear Testing*

The specimens that were subjected to wear testing are demonstrated in Figure 6a–c along with the SEM images in Figure 6d,e. The worn specimens demonstrated scattered grooves in parallel lines, which were most likely caused by abrasion due to the zirconia ball in the tribometer. The hardness of the zirconia ball was sufficient to dislodge the asperities from the surface in the form of the wear debris at the time of reciprocating movement. These asperities drag against the opposite surface and create scratches. So, abrasive wear was the predominant wear phenomenon, concurrent with the findings reported earlier by Sukhpreet et al. [8].

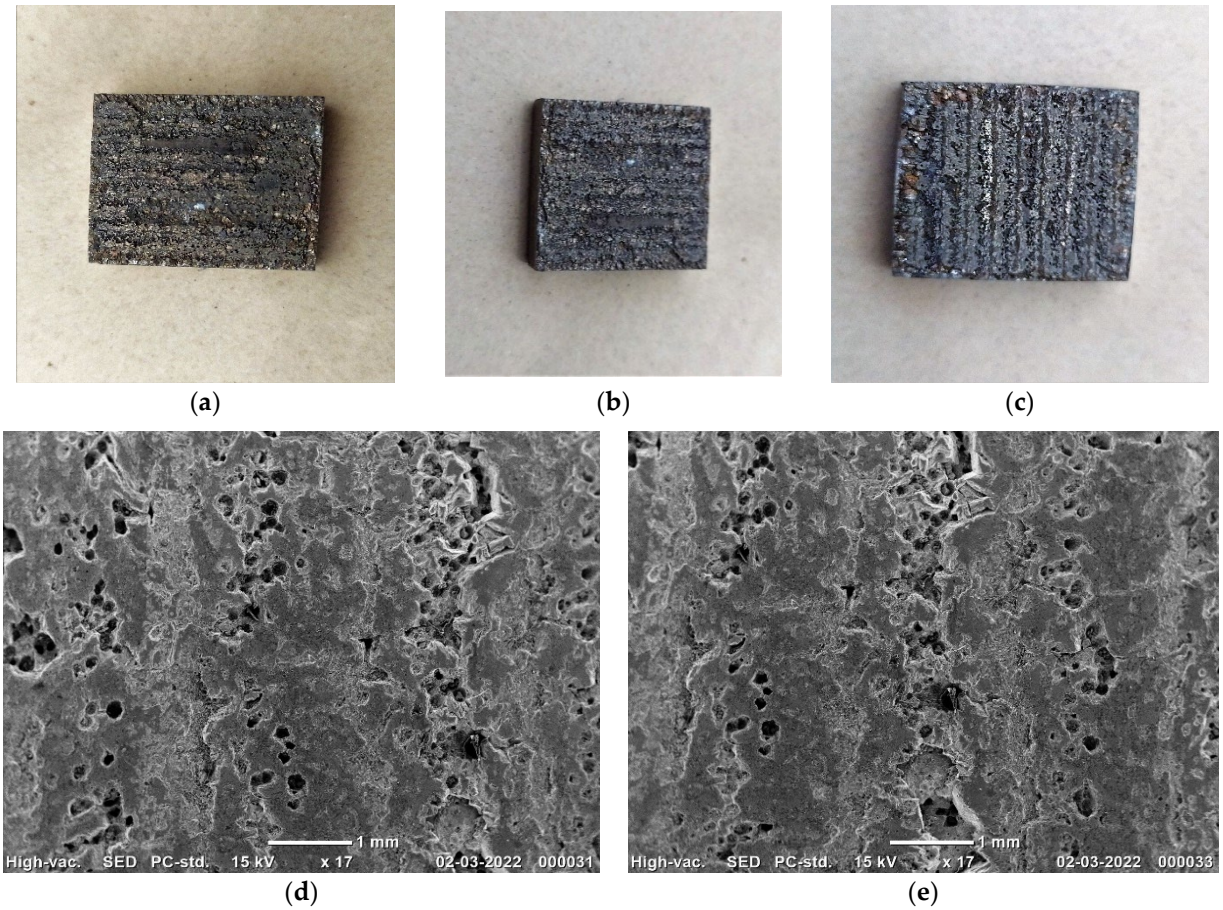


**Figure 6.** Wear tracks on (**a**–**c**) cladded specimens and (**d**,**e**) SEM images.

### *4.4. Coefficient of Friction (CoF)*

The graphs illustrated in Figure 7 a,b depict the relationship of CoF vs. time and wear vs. time.

From the graphs, it can be seen that the value of CoF increased suddenly and reached a maximum of ~0.7. This may be due to the initial stages during which the zirconia ball starts rubbing against the cladded surface, followed by dislodging the surface asperities, thereby creating more friction at the interface. After 100 s, the CoF noticeably decreased for 15 and 20 N loads and settled around 0.15. For the 10 N loading, it was observed to fluctuate around 0.3. After 200 s, the steady-state phase is achieved, and very slight changes were observed except for the 10 N load, which still showed some resistance to achieving the steady-state. This can be attributed to lower loads on the ball generating frictional force, which was not enough to break off the material from the alloy specimens. Conversely, at higher loads, the friction was high enough to break off the upper layer of the specimen, and metallic debris was generated. Upon immersion in the Ringer's solution, the debris acted

as a solid lubricant, thereby reducing the actual area of contact, ultimately responsible for the decrease in the CoF and hence the wear [17].

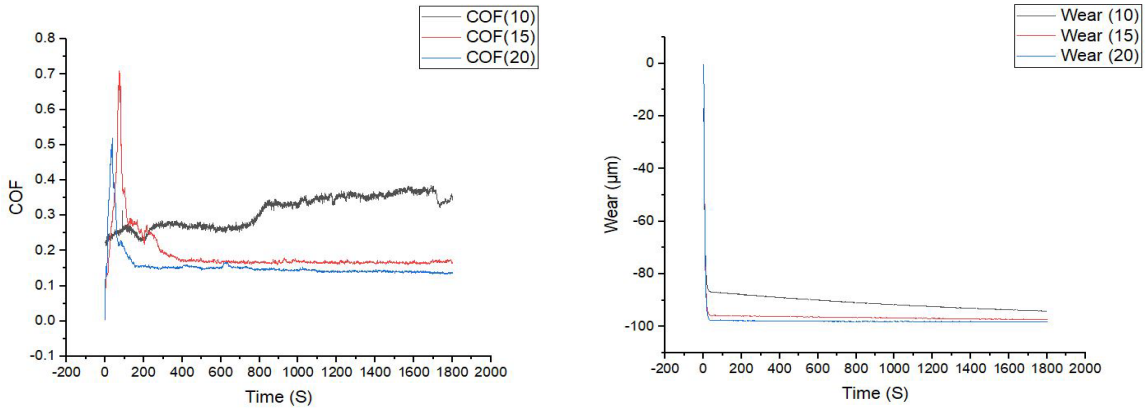


(**a**) (**b**)

**Figure 7.** Graphs of (**a**) CoF vs. time and (**b**) wear vs. time.

*4.5. Wear Rate*

The wear rate was calculated from the following equation as described by the authors of [31]:

$$\omega = \frac{V}{N \times L} \quad (2)$$

where ω is the wear rate ($mm^3/Nm$), N is the load (N), V is the wear volume ($mm^3$), and L is the sliding distance (m). The value of $V_{loss}$ was negligible in the evaluated alloy specimens. As per Archard's law, the volumetric loss of the material is inversely proportional to the hardness of the material. Materials with high hardness essentially have good wear resistance [25,33].

The calculated volume loss, wear rate, and CoF of the specimens are highlighted in Table 2.

**Table 2.** Volume loss ($V_{loss}$), wear rate, and CoF of Ti-17Nb-6Ta.

| Load (N) | Initial Weight (g) | Final Weight (g) | Wloss (g) | Density ($g/cm^3$) | Vloss ($mm^3$) | Wear Rate ($mm^3/Nm$) | CoF |
|---|---|---|---|---|---|---|---|
| 10 | 8.791 | 8.657 | 0.134 | 5.179 | 25.854 | 0.035 | 0.312 |
| 15 | 8.793 | 8.740 | 0.053 | 5.179 | 10.214 | 0.009 | 0.155 |
| 20 | 8.785 | 8.760 | 0.025 | 5.179 | 4.808 | 0.003 | 0.189 |

## 5. Conclusions

This study describes the wear characteristics of the Ti alloy Ti-17Nb-6Ta. To the best of the authors' knowledge, using laser cladding to manufacture this alloy is the first time this has been performed. The following conclusions from this study are drawn:

(1) Ti-17Nb-6Ta alloy possesses the β phase attributable to the elements Nb and Ta, which was confirmed by the XRD analysis. The β phase is deemed essential for the alloy to be compatible with biomedical applications.

(2) Abrasive wear plays a significant role in the wear mechanism. The wear rate of the specimens with 15 N (0.0045 $mm^3/Nm$) and 20 N load (0.007 $mm^3/Nm$) was relatively lower in comparison to the specimens with 10 N load (0.035 $mm^3/Nm$). The average wear rate is close to 0.016 $mm^3/Nm$.

(3) CoF was higher during the initial stages due to the surface unevenness of the alloy surface, but after 100 s, a decreasing trend was observed. After 200 s of the run, the

CoF fluctuated in a narrow range. CoF for 10 N load (0.312) was higher in comparison to 15 N (0.155) and 20 N load (0.189). The average CoF is close to 0.22.

The wear results look advantageous from this characterization. The wear rate was close to what was reported in the earlier studies [25,27]. However, this was an effort only to check out the possibility of making the alloy by laser cladding and evaluate the wear behavior. Further characterizations are necessary to evaluate its full potential to be used as an artificial joint material in artificial hip and knee joint replacements.

**Author Contributions:** Conceptualization and methodology, R.S., S.P., S.K., S.S. and H.N.; writing—original draft preparation, R.S., S.P., S.K., S.S. and H.N.; writing—review and editing, R.S., S.P., S.K., S.S. and H.M.A.M.H. All authors have read and agreed to the published version of the manuscript.

**Funding:** This research received no external funding.

**Institutional Review Board Statement:** Not applicable.

**Informed Consent Statement:** Not applicable.

**Data Availability Statement:** Not applicable.

**Acknowledgments:** Authors duly acknowledge the facilities provided by CIF, IIT-BHU, Varanasi for conducting SEM, EDX, and XRD Testing. The authors gratefully acknowledge the contribution of R K Gautam for help in the wear testing.

**Conflicts of Interest:** The authors declare that they have no conflict of interest.

## References

1. Niinomi, M. Mechanical Biocompatibilities of Titanium Alloys for Biomedical Applications. *J. Mech. Behav. Biomed. Mater.* **2008**, *1*, 30–42. [CrossRef] [PubMed]
2. Niinomi, M. Recent Research and Development in Titanium Alloys for Biomedical Applications and Healthcare Goods. *Sci. Technol. Adv. Mater.* **2003**, *4*, 445–454. [CrossRef]
3. Hussein, A.H.; Gepreel, M.A.H.; Gouda, M.K.; Hefnawy, A.M.; Kandil, S.H. Biocompatibility of New Ti-Nb-Ta Base Alloys. *Mater. Sci. Eng. C* **2016**, *61*, 574–578. [CrossRef] [PubMed]
4. Niinomi, M. Biologically and Mechanically Biocompatible Titanium Alloys. *Mater. Trans.* **2008**, *49*, 2170–2178. [CrossRef]
5. Liu, J.; Ruan, J.; Chang, L.; Yang, H.; Ruan, W. Porous Nb-Ti-Ta Alloy Scaffolds for Bone Tissue Engineering: Fabrication, Mechanical Properties and in Vitro/Vivo Biocompatibility. *Mater. Sci. Eng. C* **2017**, *78*, 503–512. [CrossRef]
6. Liu, J.; Yang, Q.; Yin, J.; Yang, H. Effects of Alloying Elements and Annealing Treatment on the Microstructure and Mechanical Properties of Nb-Ta-Ti Alloys Fabricated by Partial Diffusion for Biomedical Applications. *Mater. Sci. Eng. C* **2020**, *110*, 110542. [CrossRef]
7. Chen, Y.H.; Chuang, W.S.; Huang, J.C.; Wang, X.; Chou, H.S.; Lai, Y.J.; Lin, P.H. On the Bio-Corrosion and Biocompatibility of TiTaNb Medium Entropy Alloy Films. *Appl. Surf. Sci.* **2020**, *508*, 145307. [CrossRef]
8. Kaur, S.; Ghadirinejad, K.; Oskouei, R.H. An Overview on the Tribological Performance of Titanium Alloys with Surface Modifications for Biomedical Applications. *Lubricants* **2019**, *7*, 65. [CrossRef]
9. Kuroda, D.; Niinomi, M.; Morinaga, M.; Kato, Y.; Yashiro, T. Design and Mechanical Properties of New β Type Titanium Alloys for Implant Materials. *Mater. Sci. Eng. A* **1998**, *243*, 244–249. [CrossRef]
10. Ran, J.; Jiang, F.; Sun, X.; Chen, Z.; Tian, C.; Zhao, H. Microstructure and Mechanical Properties of Ti-6al-4v Fabricated by Electron Beam Melting. *Crystals* **2020**, *10*, 972. [CrossRef]
11. Sumitomo, N.; Noritake, K.; Hattori, T.; Morikawa, K.; Niwa, S.; Sato, K.; Niinomi, M. Experiment Study on Fracture Fixation with Low Rigidity Titanium Alloy: Plate Fixation of Tibia Fracture Model in Rabbit. *J. Mater. Sci. Mater. Med.* **2008**, *19*, 1581–1586. [CrossRef] [PubMed]
12. Choe, H.C. Nanotubular Surface and Morphology of Ti-Binary and Ti-Ternary Alloys for Biocompatibility. *Thin Solid Films* **2011**, *519*, 4652–4657. [CrossRef]
13. Geetha, M.; Singh, A.K.; Asokamani, R.; Gogia, A.K. Ti Based Biomaterials, the Ultimate Choice for Orthopaedic Implants—A Review. *Prog. Mater. Sci.* **2009**, *54*, 397–425. [CrossRef]
14. Manivasagam, G.; Dhinasekaran, D.; Rajamanickam, A. Biomedical Implants: Corrosion and Its Prevention—A Review. *Recent Patents Corros. Sci.* **2010**, *2*, 40–54. [CrossRef]
15. Zhou, Y.L.; Niinomi, M.; Akahori, T.; Fukui, H.; Toda, H. Corrosion Resistance and Biocompatibility of Ti-Ta Alloys for Biomedical Applications. *Mater. Sci. Eng. A* **2005**, *398*, 28–36. [CrossRef]
16. Wei, T.Y.; Huang, J.C.; Chao, C.Y.; Wei, L.L.; Tsai, M.T.; Chen, Y.H. Microstructure and Elastic Modulus Evolution of TiTaNb Alloys. *J. Mech. Behav. Biomed. Mater.* **2018**, *86*, 224–231. [CrossRef]

17. Lee, Y.S.; Niinomi, M.; Nakai, M.; Narita, K.; Cho, K. Differences in Wear Behaviors at Sliding Contacts for β-Type and (α + β)-Type Titanium Alloys in Ringer's Solution and Air. *Mater. Trans.* **2015**, *56*, 317–326. [CrossRef]
18. Niinomi, M.; Nakai, M.; Akahori, T. Frictional Wear Characteristics of Biomedical Ti-29Nb-13Ta-4.6Zr Alloy with Various Microstructures in Air and Simulated Body Fluid. *Biomed. Mater.* **2007**, *2*, S167. [CrossRef]
19. Cai, Z.B.; Zhang, G.A.; Zhu, Y.K.; Shen, M.X.; Wang, L.P.; Zhu, M.H. Torsional Fretting Wear of a Biomedical Ti6Al7Nb Alloy for Nitrogen Ion Implantation in Bovine Serum. *Tribol. Int.* **2013**, *59*, 312–320. [CrossRef]
20. Marin, E.; Offoiach, R.; Regis, M.; Fusi, S.; Lanzutti, A.; Fedrizzi, L. Diffusive Thermal Treatments Combined with PVD Coatings for Tribological Protection of Titanium Alloys. *Mater. Des.* **2016**, *89*, 314–322. [CrossRef]
21. Seth, S.; Jones, A.H.; Lewis, O.D. Wear Resistance Performance of Thermally Sprayed Al3Ti Alloy Measured by Three Body Micro-Scale Abrasive Wear Test. *Wear* **2013**, *302*, 972–980. [CrossRef]
22. De Souza, T.M.; Leite, N.F.; Trava-Airoldi, V.J.; Corat, E.J. Studies on CVD-Diamond on Ti6A14V Alloy Surface Using Hot Filament Assisted Technique. *Thin Solid Films* **1997**, *308–309*, 254–257. [CrossRef]
23. Ramos-Saenz, C.R.; Sundaram, P.A.; Diffoot-Carlo, N. Tribological Properties of Ti-Based Alloys in a Simulated Bone-Implant Interface with Ringer's Solution at Fretting Contacts. *J. Mech. Behav. Biomed. Mater.* **2010**, *3*, 549–558. [CrossRef]
24. Barfeie, A.; Wilson, J.; Rees, J. Implant Surface Characteristics and Their Effect on Osseointegration. *Br. Dent. J.* **2015**, *218*, E9. [CrossRef] [PubMed]
25. Khan, M.M.; Nisar, M. Effect of in Situ TiC Reinforcement and Applied Load on the High-Stress Abrasive Wear Behaviour of Zinc–Aluminum Alloy. *Wear* **2022**, *488–489*, 204082. [CrossRef]
26. Jing, Z.; Cao, Q.; Jun, H. Corrosion, Wear and Biocompatibility of Hydroxyapatite Bio-Functionally Graded Coating on Titanium Alloy Surface Prepared by Laser Cladding. *Ceram. Int.* **2021**, *47*, 24641–24651. [CrossRef]
27. Dittrick, S.; Balla, V.K.; Bose, S.; Bandyopadhyay, A. Wear Performance of Laser Processed Tantalum Coatings. *Mater. Sci. Eng. C* **2011**, *31*, 1832–1835. [CrossRef] [PubMed]
28. Amado, J.M.; Rodríguez, A.; Montero, J.N.; Tobar, M.J.; Yáñez, A. A Comparison of Laser Deposition of Commercially Pure Titanium Using Gas Atomized or Ti Sponge Powders. *Surf. Coat. Technol.* **2019**, *374*, 253–263. [CrossRef]
29. Dobbelstein, H.; Gurevich, E.L.; George, E.P.; Ostendorf, A.; Laplanche, G. Laser Metal Deposition of Compositionally Graded TiZrNbTa Refractory High-Entropy Alloys Using Elemental Powder Blends. *Addit. Manuf.* **2019**, *25*, 252–262. [CrossRef]
30. Bhardwaj, T.; Shukla, M.; Paul, C.P.; Bindra, K.S. Direct Energy Deposition-Laser Additive Manufacturing of Titanium-Molybdenum Alloy: Parametric Studies, Microstructure and Mechanical Properties. *J. Alloys Compd.* **2019**, *787*, 1238–1248. [CrossRef]
31. Singh, R.; Kurella, A.; Dahotre, N.B. Laser Surface Modification of Ti-6Al-4V: Wear and Corrosion Characterization in Simulated Biofluid. *J. Biomater. Appl.* **2006**, *21*, 49–73. [CrossRef] [PubMed]
32. Kang, S.; Tu, W.; Han, J.; Li, Z.; Cheng, Y. A Significant Improvement of the Wear Resistance of Ti6Al4V Alloy by a Combined Method of Magnetron Sputtering and Plasma Electrolytic Oxidation (PEO). *Surf. Coatings Technol.* **2019**, *358*, 879–890. [CrossRef]
33. Fellah, M.; Labaïz, M.; Assala, O.; Dekhil, L.; Taleb, A.; Rezag, H.; Iost, A. Tribological Behavior of Ti-6Al-4V and Ti-6Al-7Nb Alloys for Total Hip Prosthesis. *Adv. Tribol.* **2014**, *2014*, 451387. [CrossRef]